

ChemComm

Accepted Manuscript



This article can be cited before page numbers have been issued, to do this please use: X. Yang, Y. Zhou, X. Zhang, S. Yang, Y. Chen, J. Guo, X. Li, Z. Qing and R. Yang, *Chem. Commun.*, 2016, DOI: 10.1039/C6CC05254A.



This is an *Accepted Manuscript*, which has been through the Royal Society of Chemistry peer review process and has been accepted for publication.

Accepted Manuscripts are published online shortly after acceptance, before technical editing, formatting and proof reading. Using this free service, authors can make their results available to the community, in citable form, before we publish the edited article. We will replace this *Accepted Manuscript* with the edited and formatted *Advance Article* as soon as it is available.

You can find more information about *Accepted Manuscripts* in the [Information for Authors](#).

Please note that technical editing may introduce minor changes to the text and/or graphics, which may alter content. The journal's standard [Terms & Conditions](#) and the [Ethical guidelines](#) still apply. In no event shall the Royal Society of Chemistry be held responsible for any errors or omissions in this *Accepted Manuscript* or any consequences arising from the use of any information it contains.

Journal Name

COMMUNICATION

A TP-FRET-Based Two-Photon Fluorescent Probe for Ratiometric Visualization of Endogenous Sulfur Dioxide Derivatives in Mitochondria of Living Cells and Tissues†

 Received 00th January 20xx,
Accepted 00th January 20xx

DOI: 10.1039/x0xx00000x

 Xiaoguang Yang,^{a§} Yibo Zhou,^{b§} Xiufang Zhang,^b Sheng Yang,^{*a} Yun Chen,^b Jingru Guo,^a Xiaoxuan Li,^a Zhihe Qing,^a and Ronghua Yang^{*ab}

www.rsc.org/

A ratiometric two-photon fluorescent probe for SO₂ derivatives was first proposed based on acedan-merocyanine dyads via TP-FRET strategy. It was successfully applied to visualizing of the fluctuations of enzymatically generated SO₂ derivatives in mitochondria of HepG2 cells and rat liver tissues by two-photon fluorescence microscopy imaging.

Sulfur dioxide (SO₂) was traditionally considered as a kind of environmental pollutant,¹ since studies have implied that exposure to SO₂ was usually associated with the symptoms of neurological disorders, cardiovascular diseases, and even lung cancer.² However, SO₂ has recently emerged as an important gasotransmitter due to it possesses some beneficial biological functions including antioxidation and cardiovascular regulation.³ Interestingly, it is reported that SO₂ can be endogenously produced from sulfur-containing amino acids, equilibrating with sulfites/bisulfites (HSO₃⁻/SO₃²⁻) in biosystems.⁴ Therefore, it is meaningful and valuable to detailedly elucidate the generation and physiological roles of SO₂ and its derivatives using an effective molecular tool.

Fluorescent probe in combination with imaging instruments offers a powerful approach for in situ and real-time visualizing biomolecules of interest in living organisms, owing to its non-invasiveness and high spatiotemporal resolution.⁵ Because mitochondria is the main region of endogenous SO₂ derivatives formation,⁶ a selective, fast response and targetable fluorescent probe for exploring SO₂ biology in mitochondria is especially appreciated. Although considerable advances in the development of fluorescent probes for SO₂ derivatives have been made in recent years,⁷ so far, only a few ones are mitochondria-targeted.⁸ Nevertheless, all of them are

restricted by one photon excitation with wavelengths in the ultraviolet-visible (UV/Vis) spectral region, which renders them can only be employed in cellular level but difficult for complicated living systems, because well absorbance, easy scattering and strong autofluorescence in the short wavelength region elicits high background noise and poor tissue penetration.⁹

To address above issues, two-photon microscopy (TPM), utilizing two near-infrared photons with low energy as the exciting light, has become a potent alternative technique for biomedical applications,¹⁰ because it provides improved three-dimensional spatial localization with minimized background signal, deeper tissue penetration, and reduced photodamage to biosamples.¹¹ Despite all these advantages, only one example of two-photon probe for fluorescent imaging mitochondrial SO₂ derivatives in tissues has been judiciously designed by Chao et al until recently.¹² However, its detecting signal relied on single-emission intensity changes, which would easily suffer the external interferences from instrumental efficiency, probe distribution, and local surrounding.¹³ In sharp contrast, ratiometric probes can provide self-calibration for the aforementioned factors and thus enable more accurate analysis through measuring ratio variations of two emission intensities at different wavelengths.¹⁴ It is worth pointing out that, as far as we know, no ratiometric two-photon fluorescent probe for visualizing mitochondrial SO₂ derivatives in tissues has been reported hitherto.

By virtue of the dual superiorities of the TPM technique and the ratiometric mode, herein, we firstly proposed a mitochondria-targetable and ratiometric two-photon fluorescent probe, TP-Mito/Ratio-SO₂, for SO₂ derivatives imaging via two-photon excited fluorescence resonance energy transfer (TP-FRET) strategy. As briefly depicted in Scheme 1, TP-Mito/Ratio-SO₂ was rationally constructed based on an acedan-merocyanine scaffold as energy transfer cassette. Under two-photon excitation condition, the energy transfer dyad would fluoresce at the characteristic emission of merocyanine due to appropriate spectrum matching between absorption spectra of acceptor with two-photon emission

^aSchool of Chemistry and Biological Engineering, Changsha University of Science and Technology, Changsha, 410114, China.

E-mail: ysh1127@hnu.edu.cn, yangrh@pku.edu.cn. Tel/Fax: +86 731-88822523.

^bState Key Laboratory of Chemo/Biosensing and Chemometrics, College of Chemistry and Chemical Engineering, Hunan University, Changsha 410082, China.

[§]These authors contributed equally.

†Electronic Supplementary Information (ESI) available: Experimental details, synthesis and characterization of compound, and other data noted in the text. See DOI: 10.1039/x0xx00000x

spectra of donor (Fig. S1). However, the conjugation structure of TP-Mito/Ratio-SO₂ would be disturbed by nucleophilic addition of HSO₃⁻/SO₃²⁻ toward merocyanine, impeding the TP-FRET process and thus resulting in fluorescence recovery of acedan dye. The design rationality was supported by density functional theory (DFT) calculations (Fig. S2).



Scheme 1 Response Mechanism of TP-Mito/Ratio-SO₂ toward SO₂ Derivatives

TP-Mito/Ratio-SO₂ was efficiently synthesized and characterized as described in the Electronic Supplementary Information. With the probe in hand, we start to investigate its photophysical properties and response abilities toward HSO₃⁻/SO₃²⁻. As shown in Fig. 1A, the absorption spectra of free probe in buffer solution exhibited strong electronic transitions at 380 nm and 510 nm ($\epsilon_{380} = 2.1 \times 10^4 \text{ M}^{-1} \text{ cm}^{-1}$, $\epsilon_{510} = 5.3 \times 10^4 \text{ M}^{-1} \text{ cm}^{-1}$), which are assigned to the characteristic absorption of acedan and merocyanine derivative respectively, indicating that there are little or no electronic interactions between the energy transfer dyad in the ground state. Upon addition of increasing concentrations of NaHSO₃, the probe's absorption peak gradually attenuated concomitant with a color change from red to colourless (inset of Fig. 1A), revealing that it could response to SO₂ derivates. Mass data (new peak appeared at *m/z* 715) and disappearance of the resonance signal corresponding to the alkene proton in partial ¹H NMR also provide the evidence of addition reaction between TP-Mito/Ratio-SO₂ and NaHSO₃ (Fig. S3,S4).

To evaluate the sensing performances of TP-Mito/Ratio-SO₂, fluorometric titration of the probe toward different concentrations of NaHSO₃ in buffer solution were first carried out. As shown in Fig. 1B, under one-photon ($\lambda_{\text{ex}} = 380 \text{ nm}$) excitation, the free probe exhibits slight characteristic emission peak of acedan but strong fluorescence emission of merocyanine at 590 nm. With the increasing concentration of NaHSO₃, there is significant decrease in characteristic emission of merocyanine and a blue-shifted center around 500 nm appears with around 90 nm emission shift and a clear iso-emission point at 560nm. Observably, a signal to background ratio, *S/B* ($S/B = [F_{500}/F_{590}]_n / [F_{500}/F_{590}]_0$),¹⁵ was increased from 1.0 to 6.5 when treated with 40.0 μM NaHSO₃ (Fig. S5). Moreover, there was a well linear relationship between the *S/B* and the concentrations of NaHSO₃ in the range from 0 to 10.0 μM with a detection limit ($3\sigma/\text{slope}$) of 50 nM, demonstrating that TP-Mito/Ratio-SO₂ is potentially suitable for quantitative determination of HSO₃⁻/SO₃²⁻ concentrations.

Real time fluorescence records and kinetic studies of TP-Mito/Ratio-SO₂ in response to different concentrations of NaHSO₃ were then performed. As shown in Fig. S6, the emission intensity ratio, F_{500}/F_{590} , gradually increased with time and reached a maximum plateau in about 3 min after treatment with 40.0 μM NaHSO₃ solution, such a rapid response is appealing for real-time detection. However, the free probe showed no detectable change with time, demonstrating that the probe was stable under aqueous

solution. The time-dependent processes for different concentrations of NaHSO₃ followed first-order kinetics with diverse observed rate constant *k'* ($k'_{\text{max}} = 1.2 \times 10^{-2} \text{ s}^{-1}$, Fig. S7). Moreover, a linear relation between the *k'* with NaHSO₃ passing through the origin can be found, which indicates that the reaction was second-order overall for TP-Mito/Ratio-SO₂ and NaHSO₃ with $k = 297 \text{ M}^{-1} \text{ s}^{-1}$ (Inset of Fig. S7).¹⁶

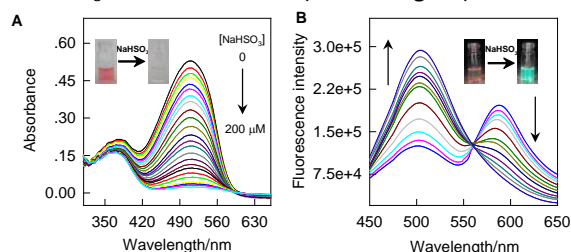


Fig. 1 (A) UV-vis absorption spectra of TP-Mito/Ratio-SO₂ (10.0 μM) in the presence of different amounts of NaHSO₃ in PB solution (pH = 7.4, containing 20% EtOH), Inset: color change of TP-Mito/Ratio-SO₂ after treatment with NaHSO₃; (B) Fluorescence response of TP-Mito/Ratio-SO₂ (5.0 μM) to NaHSO₃ (0-40.0 μM) in PB solution (pH = 7.4, containing 20% EtOH). $\lambda_{\text{ex}} = 380 \text{ nm}$. Inset: fluorescence change of TP-Mito/Ratio-SO₂ after treatment with NaHSO₃.

To evaluate the selectivity performance of this new probe, fluorometric titrations for TP-Mito/Ratio-SO₂ were extended to various bio-relevant species including common anions (F⁻, Cl⁻, Br⁻, I⁻, AcO⁻, HCO₃⁻, SCN⁻, CN⁻, SO₄²⁻), representative reactive oxygen and nitrogen species (H₂O₂, NO), and other reactive sulfur species (S₂O₃²⁻, HS⁻, Cys, Hcy, and GSH). Fig. S8 depicted that no significant variation could be found in the presence of aforementioned competitive substrates other than HSO₃⁻/SO₃²⁻, indicating that TP-Mito/Ratio-SO₂ could selectively response toward SO₂ derivates. Furthermore, competition experiments depicted that this probe could specifically react with SO₂ derivates in the presence of other potentially competitive species, which is helpful in validation of the designed probe to meet the demands of selectivity for SO₂ derivates assay in biological applications.

Effect of pH on the fluorescence properties of TP-Mito/Ratio-SO₂ and its response toward SO₂ derivates were subsequently investigated (Fig. S9). The free probe was pH insensitive in the broad pH range (4.0-10.0), demonstrating that the probe was steady at physiological pH conditions. Upon treatment with HSO₃⁻, the maximal emission intensity ratio was observed in the pH range of 8.0-11.0, suggesting that the two-photon ratiometric probe functions properly at physiological pH. There was a drastic downward trend in response signal at pH values changing from 8.0 to 6.0, which was in accordance with the $\text{pK}_{\text{a}2}$ of HSO₃⁻ ($\text{pK}_{\text{a}2} = 7.20$),¹⁷ indicating that protonation of HSO₃⁻ lessen its nucleophilicity to the acceptor unit of TP-Mito/Ratio-SO₂ under acidic condition.

The two-photon excitation action cross-section ($\Phi\delta$) is one of pivotal parameter for a admirable two photon bioimaging probe. Particularly noteworthy is the fact that the maximum $\Phi\delta$ values of both TP-Mito/Ratio-SO₂ and its reaction product with NaHSO₃ were near 100 GM at 760 nm (Fig. S10), demonstrating that the maximum two-photon excitation wavelength of the energy donor portions remains stationary, which is significantly superior for TP ratiometric imaging than

ICT based ones.¹⁸ Meanwhile, under the optimum two-photon irradiation (760 nm), two-photon fluorescence emission spectra of the probe and its reaction product with NaHSO_3 are similar as their one-photon based ones (Fig. S11), impressively, emission intensity at 590 nm of TP-Mito/Ratio-SO₂ is about 5-fold brighter than that of free acceptor, confirming that TP-FRET process from acedan to merocyanine occurs.

The excellent two-photon properties and response performances in vitro of probe encourage us to explore whether TP-Mito/Ratio-SO₂ could function in mitochondria of living systems. Before bioimaging experiments, the cytotoxicities of TP-Mito/Ratio-SO₂ on HepG2 cells were primarily evaluated by standard MTT assay (Fig. S12). After cells were treated with TP-Mito/Ratio-SO₂ (0–30 μM) for 24 h, a high cell survive rate (> 90%) can be found. The low cytotoxic effect of the candidate probe is well suitable for bioimaging application. Subsequently, TPM imaging of living cells were carried out on confocal laser scanning microscopy. As described in Fig. S13, HepG2 cells incubated with 5.0 μM TP-Mito/Ratio-SO₂ show fluorescence in red channels, but there is negligible fluorescence signal through green channels. On the contrary, the probe-loaded cells appear clear cellular profiles with brighter green fluorescence when treated with the increase of NaHSO_3 for 10 min, the original fluorescence signal in the red channel gradually weakened accordingly. These imaging results indicate that TP-Mito/Ratio-SO₂ shows good cell-permeability and can be applied to dual-colour monitor the variations in concentrations of SO₂ derivatives in living cells.

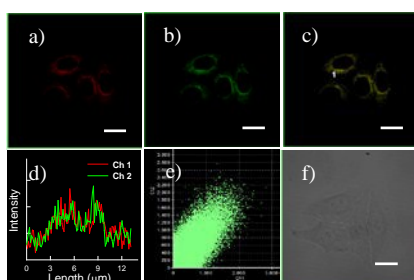


Fig. 2 Fluorescence images of TP-Mito/Ratio-SO₂ colocalizes to the mitochondria in HepG2 cells. Cells were stained with (a) TP-Mito/Ratio-SO₂ (5.0 μM , Channel 1 (red), λ_{ex} = 405 nm; λ_{em} = 580–630 nm) and (b) MitoTracker Green FM (1.0 μM , Channel 2 (green), λ_{ex} = 488 nm; λ_{em} = 500–530 nm) simultaneously. (c) The merged pattern of a and b. (d) intensity profile of ROI cross the HepG2 cell costained with TP-Mito/Ratio-SO₂ and MitoTracker Green FM. (e) Intensity scatter plot of two channels. (f) bright field pattern of cells. Scale bar: 10 μm .

similar as well-known mitochondria-targetable cationic dyes including cyanine and rhodamine, TP-Mito/Ratio-SO₂ also possess an overall positive charge, speculating that the designed probe would accumulated in the mitochondria. In order to determine its subcellular localization, colocalization experiments were conducted by costaining HepG2 cells with a commercially mitochondrial tracker MitoTracker Green FM and TP-Mito/Ratio-SO₂ (Fig. 2). These cells appear red and green fluorescences in Channel 1 (Fig. 2a) and Channel 2 (Fig. 2b), respectively. The merged image (Fig. 2c) reveals that the staining of TP-Mito/Ratio-SO₂ overlays well with that of MitoTracker Green FM. The variations in intensity profile of linear regions of interest (ROI) across cell in the two channels

show tendency to synchrony (Fig. 2d). Moreover, the intensity scatter plot is high correlation with Pearson's colocalization coefficient 0.95 (Fig. 2e). The above investigations confirmed that TP-Mito/Ratio-SO₂ could specifically accumulate in mitochondria.

Mitochondria localization feature of TP-Mito/Ratio-SO₂ actuate us to test its imaging performances toward endogenous SO₂ derivatives. As we known, SO₂ derivatives can be endogenously generated from reaction of $\text{Na}_2\text{S}_2\text{O}_3$ and GSH catalyzed by thiosulphate sulphurtransferase (TST) in mammals. Previous studies also demonstrated that liver injury arised from oxidative stress can lead to depletion of abundant GSH.¹⁹ Therefore, to testify our assumption, the human hepatoma cell line (HepG2) were treated with exogenous GSH and $\text{Na}_2\text{S}_2\text{O}_3$ as TST substrates in the absence and presence of TST inhibitor SNAP for cellular imaging experiments²⁰. One can find in Fig. 3 that, in comparison with the free probe loaded cells, similar imaging patterns could be observed from probe-loaded cells in the presence of $\text{Na}_2\text{S}_2\text{O}_3$ and GSH individually. By contrast, there was obviously increasing fluorescence signal in green channels concomitant with decrease of fluorescence signal in red channels for the probe-treated cells with the presence of both $\text{Na}_2\text{S}_2\text{O}_3$ and GSH, resulting in prominent fluorescence ratio signal change (Fig. 3D). Moreover, even though simultaneous treatment with $\text{Na}_2\text{S}_2\text{O}_3$ and GSH, there was still no significant fluorescence change when probe-loaded HepG2 cells were pre-incubated with TST inhibitor SNAP (Fig. 3E), confirming that the fluorescence changes were indeed initiated from endogenously generated $\text{HSO}_3^-/\text{SO}_3^{2-}$. These results strongly suggest that that TP-Mito/Ratio-SO₂ was suitable for visualizing changes of endogenous SO₂ derivatives inside HepG2 cells.

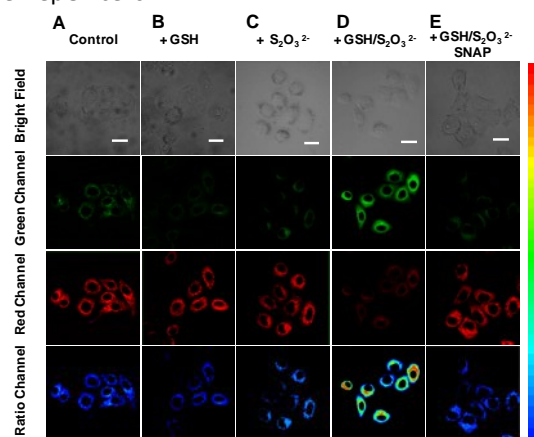


Fig. 3 Two-photon ratiometric fluorescence images of endogenous SO₂ derivatives in mitochondria of HepG2 cells using 5.0 μM TP-Mito/Ratio-SO₂ under different conditions: (A) the probe only. (B) in the presence of 500 μM GSH. (C) in the presence of 250 μM $\text{Na}_2\text{S}_2\text{O}_3$. (D) in the presence of TST substrates 250 μM /500 μM $\text{Na}_2\text{S}_2\text{O}_3$ /GSH. (E) 100 nM SNAP solution was pre-incubated with HepG2 cells, and then treated with the probe in the presence of 250 μM $\text{Na}_2\text{S}_2\text{O}_3$ and 500 μM GSH. Scale bar: 20 μm .

To further display the advantage of TPM, immediately after cellular imaging experiments, we proceeded to investigate the utility of the probe for monitoring endogenous SO₂ in deep-tissue imaging. Because high levels of GSH are conserved in

normal hepatocytes,²⁰ two-photon ratiometric imaging of TP-Mito/Ratio-SO₂ in fresh rat liver tissue slices were carried out under different conditions from cellular ones. As is shown in Fig. 4A, the tissue treated with probe showed weak fluorescence signal in green channels but strong fluorescence signal in red channels. Moreover, Z-scan mode revealed that the fluorescence signals were collected at different tissue depths (0–200 μm), as depicted in Fig. S14, suggesting that TP-Mito/Ratio-SO₂ could be successfully applied for deep-tissue imaging. Difference from the free probe-loaded tissue, the fluorescence intensity in green channel slightly enhanced along with faint signal decrease in the red channel for probe-loaded cells in the presence of Na₂S₂O₃, thus a certain change of ratiometric pattern could be observed (Fig. 4B). In sharp contrast, the fluorescence ratio of the control ones increased dramatically upon treatment with α-lipoic acid (GSH stimulator) and decreased significantly when dealing with N-ethylmaleimide (NEM, a well-known biothiols scavenger) (Fig. 4C,D), meaning that enzymatically generated SO₂ derivates in tissues really originate from the interaction of Na₂S₂O₃ and endogenous GSH. What is more, when the tissue was pre-treated with SNAP to invalidate catalytic activity of TST, ratiometric fluorescence changes would disappear (Fig. 4E). These imaging findings demonstrate that TP-Mito/Ratio-SO₂ can effectively enable the determination of endogenous SO₂ fluctuation at depths in rat live tissues using TPM.

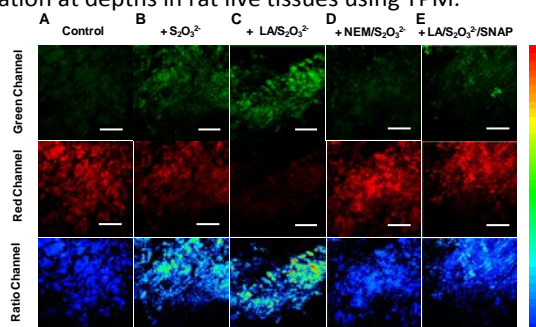


Fig. 4 Two-photon fluorescence images of endogenous SO₂ derivates in mitochondria of fresh rat liver tissues at depth of 120 μm using 50 μM TP-Mito/Ratio-SO₂ under different conditions: (A) the probe only. (B) in the presence of 2.5 mM Na₂S₂O₃. (C) in the presence of 2.5 mM Na₂S₂O₃ and 5.0 mM α-lipoic acid. (d) in the presence of 2.5 mM Na₂S₂O₃ and 10.0 mM NEM. (e) For the control experiments, 2 μM SNAP solution was pre-incubated with tissue, and then treated with the probe in the presence of 2.5 mM Na₂S₂O₃ and 5.0 mM α-lipoic acid. Scale bar: 50 μm.

In summary, we have constructed a mitochondria-targetable and ratiometric two-photon fluorescence imaging probe for SO₂ derivates based on acedan-merocyanine dyads for the first time. This probe, designed with the aim of modulating two-photon fluorophore with energy acceptor via TP-FRET process, exhibits a significant red-to-green fluorescence color change in response to SO₂ derivates with excellent features including high TP cross section, fast response, good selectivity, and robust staining ability of mitochondria, thereby allowing ratiometric visualization of the variation of SO₂ derivates in mitochondria of living cells and deep tissues. More importantly, the ratiometric TPM imaging studies clearly reveal the endogenous SO₂ derivates within mitochondria of living

systems with respect to the enzymatic reaction of Na₂S₂O₃ and GSH, demonstrating that the newly proposed probe will be an effective molecule tool to study metabolism of sulfur-containing species in biomedical research.

The authors would like to acknowledge the financial support from NSFC (21505006, 21135001, 21575018, 21521063) and the Open Funds of State Key Laboratory of Chemo/Biosensing and Chemometrics of Hunan University (2015011).

Notes and references

- 1 T. M. Chen, J. Gokhale, S. Shofer and W. G. Kuschner, *Am J Med Sci.*, 2007, **333**, 249.
- 2 N. Sang, Y. Yun, H. Li, L. Hou, M. Han and G. K. Li, *Toxicol. Sci.*, 2010, **114**, 226.
- 3 (a) Y. Liang, D. Liu, T. Ochs, C. Tang, S. Chen and S. Zhang, *Lab. Invest.*, 2011, **91**, 12.; (b) K. D. Hu, G. S. Bai, W. J. Li, H. Yan, L. Y. Hu, Y. H. Li and H. Zhang, *Plant. Growth. Regul.*, 2015, **75**, 271.; (c) Z. Meng, Y. Li and J. Li, *Arch. Biochem. Biophys.*, 2007, **467**, 291.; (d) Z. Q. Meng, Z. H. Yang, J. L. Li and Q. X. Zhang, *Chemosphere.*, 2012, **89**, 579.
- 4 L. Luo, S. Chen, H. Jin, C. Tang and J. Du, *Biochem. Biophys. Res. Commun.*, 2011, **415**, 61.
- 5 J. Chan, S. C. Dodani, C. J. Chang, *Nat. Chem.*, 2012, **4**, 973.
- 6 T. Ubuka, S. Yuasa, J. Ohta, N. Masuoka, K. Yao and M. Kinuta, *Acta medica Okayama.*, 1990, **44**, 55.
- 7 (a) G. Li, Y. Chen, J. Wang, Q. Lin, J. Zhao, L. Ji and H. Chao, *Chem. Sci.*, 2013, **4**, 4426; (b) Y. Q. Sun, J. Liu, J. Zhang, T. Yang and W. Guo, *Chem. Commun.*, 2013, **49**, 2637. (c) X. Cheng, H. Jia, J. Feng, J. Qin and Z. Li, *J. Mater. Chem. B.*, 2013, **1**, 4110; (d) M. Y. Wu, K. Li, C. Y. Li, J. T. Hou and X. Q. Yu, *Chem. Commun.*, 2014, **50**, 183; (e) W. Chen, Q. Fang, D. Yang, H. Zhang, X. Song and J. Foley, *Anal. Chem.*, 2015, **87**, 609; (f) L. Zhu, J. Xu, Z. Sun, B. Fu, C. Qin, L. Zeng and X. Hu, *Chem. Commun.*, 2015, **51**, 1154.
- 8 (a) W. Xu, C. L. Teoh, J. Peng, D. Su, L. Yuan and Y. T. Chang, *Biomaterials.*, 2015, **56**, 1; (b) J. Xu, J. Pan, X. Jiang, C. Qin, L. Zeng, H. Zhang, J. F. Zhang, *Biosens. Bioelectron.*, 2016, **77**, 725. (c) Y. Liu, K. Li, M. Y. Wu, Y. H. Liu, Y. M. Xie and X. Q. Yu, *Chem. Commun.*, 2015, **51**, 10236. (d) D. P. Li, Z. Y. Wang, X. J. Cao, J. Cui, X. Wang, H. Z. Cui, J. Y. Miao and B. X. Zhao, *Chem. Commun.*, 2016, **52**, 2760.
- 9 Z. Chen, H. Chen, H. Hu, M. Yu, F. Li, Q. Zhang, Z. Zhou, T. Yi and C. Huang, *J. Am. Chem. Soc.*, 2008, **130**, 3023.
- 10 H. M. Kim and B. R. Cho, *Chem. Rev.*, 2015, **115**, 5014.
- 11 (a) L. Guo, and M. S. Wong, *Adv. Mater.*, 2014, **26**, 5400; (b) H. Yan, L. He, C. Ma, J. Li, J. Yang, R. Yang and W. Tan, *Chem. Commun.*, 2014, **50**, 8398.
- 12 G. Li, Y. Chen, J. Wang, J. Wu, G. Gasser, L. Ji and H. Chao, *Biomaterials.*, 2015, **63**, 128.
- 13 Z. C. Xu, K. H. Baek, H. N. Kim, J. N. Cui, X. H. Qian, D. R. Spring, I. J. Shin, J. Y. Yoon, *J. Am. Chem. Soc.*, 2010, **132**, 601.
- 14 L. Zhou, X. Zhang, Q. Wang, Y. Lv, G. Mao, A. Luo, Y. Wu, Y. Wu, J. Zhang and W. Tan, *J. Am. Chem. Soc.*, 2014, **136**, 9838.
- 15 J. Zheng, J. Li, X. Gao, J. Jin, K. Wang, W. Tan and R. Yang, *Anal. Chem.*, 2010, **82**, 3914.
- 16 C. S. Lim, G. Masanta, H. J. Kim, J. H. Han, H. M. Kim and B. R. Cho, *J. Am. Chem. Soc.*, 2011, **133**, 11132.
- 17 M. Sun, H. Yu, K. Zhang, Y. Zhang, Y. Yan, D. Huang and S. Wang, *Anal. Chem.*, 2014, **86**, 9381.
- 18 L. Yuan, F. P. Jin, Z. B. Zeng, C. B. Liu, S. L. Luo and J. S. Wu, *Chem. Sci.*, 2015, **6**, 2360.
- 19 B. Tang, Y. L. Xing, P. Li, N. Zhang, F. B. Yu and G. W. Yang, *J. Am. Chem. Soc.*, 2007, **129**, 11666.
- 20 I. Kwiecień, M. Sokołowska, E. Luchter-Wasylewska and L. Włodek, *Int. J. Biochem. Cell. Biol.*, 2003, **35**, 1645.